Final version published in *Canadian Journal of Chemistry*, v.102, n.4 (2024).
https://doi.org/10.1139/cjc-2023-0145

Cross-Linked Polymer Film on Copper Stubs as a Reusable Substrate Enabling Imaging and Quantitative Analyses of Aluminosilicate Particles

Taylor Filewood, Alex J. G. Rea, Gurbinder Kaur, Annabelle M. K. Hadley, George Agnes, and Byron D. Gates *

Department of Chemistry
Simon Fraser University
8888 University Drive
Burnaby, BC V5A 1S6 (Canada)
Telephone Number: (778) 782-8066
Fax Number: (778) 782-3765
*Email Address: bgates@sfu.ca

Abstract

Access issues to potable waters around the planet is the motivation for research in desalination technologies. One class of materials that is a research focus for desalination membranes are zeolites that are comprised of silicon, aluminum, and oxygen, and have structures that include regular pores of varying sizes dependent on the type of zeolite. A motivation for this study was to enable characterization of non-conductive materials containing silicon or aluminum (e.g., zeolites) using scanning electron microscopy (SEM) and energy dispersive X-ray spectroscopy (EDS) techniques. To avoid significant background signals directly overlapping with these samples, common sample supports and preparation protocols involving aluminum or silicon were precluded. Cross-linked polymer coatings applied via spin coating onto polished copper (Cu) stubs are shown to be durable for reuse even with the use of aggressive cleaning techniques between samples. SEM and EDS analyses of Cu stubs were performed before and after applying the polymer coating, after drop-cast application of zeolite particles and after their subsequent removal by sonication-based techniques. The data from those trials confirmed there was no background interference from silicon or aluminum and no cross-contamination between samples during these analyses, enabling quantitation of Al and Si in the samples.

Keywords: zeolite, electron microscopy, nanoparticles, cross-linked polymer film, spin coat, reusable substrates

1. Introduction

Select synthetic approaches of preparing custom zeolite materials have demonstrated the potential for their use as tunable filtration membranes.[1-8] Zeolite crystals have regular pores, some of which can accommodate water molecules while physically restricting hydrated ions and other small molecules. The development of zeolites and strategies to generate zeolite-based membranes for potential utility in desalination applications motivates the characterization methods developed herein. One approach to exploring engineering structures of zeolites for desalination is the formation of thin sheets of zeolites created from an exfoliation of zeolite-based nanoparticles.[4,8-11] The tuning of material structural properties, and in this example, from zeolite starting materials and thin sheets generated from them, such as their dimensions and morphologies, requires access to appropriately sensitive techniques at each step of the process.

One toolbox that could be indispensable in learning how to adjust the synthesis conditions to achieve specific properties in the products, is electron-based imaging techniques.[1-8,12-17] Scanning electron microscopy (SEM) can provide information on the size and shape of individual zeolite particles. Energy dispersive X-ray spectroscopy (EDS) is used to determine the elemental composition of individual particles, which can complement bulk analysis techniques of zeolite materials such as X-ray diffraction, porosimetry measurements, and bulk elemental analysis techniques. These microscopy and spectroscopy techniques are, however, not typically used for silicon and aluminum based non-conductive materials because of background signals from materials used in processing samples and sample-support materials.

Herein, a method is described that enables the use of electron microscopy-based techniques for quantitative and qualitative analysis of silicon and aluminum containing nanomaterials, as demonstrated using individual zeolite particles. Although SEM techniques are routinely used in

these types of analyses, the use of EDS has additional challenges as summarized below that must be overcome to be more widely used in the analysis of zeolite materials.[16,17] Zeolites are an example of a non-conductive sample that must be placed on a conductive substrate. For reasons of practicality, the substrate must also be easily inserted into the sample handling apparatus of a SEM. A highly conductive substrate prevents charge accumulation on a non-conductive sample that would otherwise interfere with analysis under the focused electron beam by degrading or precluding the evaluation of sample topography and composition. The substrate must also have distinct surface characteristics so it can be differentiated from the sample materials, and not interfere with the elemental analysis of the sample composition by EDS.[16,17] Many sample holders commonly used in SEM contain aluminum or silicon. Therefore, the characterization of samples, such as zeolites, necessarily requires non-common sample holders and sample handling methods.[1-8,16,17] These are important characterization criteria because zeolite nomenclature is defined in part by an accurate measurement of its silicon to aluminum mole ratio (Si:Al). The Si:Al ratio impacts the mesoporous structure of the ZSM-5 zeolites, which are specifically fabricated and used for methanol aromatization, alkane monomolecular cracking, and separations.[18,19] It is for this reason that commonly used substrates (e.g., polished silicon wafers) were deemed to be non-viable for the characterization of zeolite particles.[17] Likewise, commonly used sample holders, termed stubs, composed of aluminum (Al) metal, cannot be used without modification of the stub.[12-15] An alternative approach has been reported, wherein zeolite samples were themselves modified by a coating that increased their electrical conductivity and improved their adhesion to the surfaces of an Al stub. Background signals from the Al in the stub were, however, present in all data sets acquired on these samples.[12-15]

In an approach to minimization of background Al signal in this study, conductive double-sided carbon tape was applied to Al stubs and zeolite particles were applied to the exposed side of the adhesive. This approach proved unsatisfactory because of the irregular thickness of the tape and the difficulty of discerning the particles from the rough topography of the tape. These factors negatively impacted the SEM image quality, and Si and Al contaminants in the carbon adhesive tape generated variations in elemental composition at different locations on a single piece of tape.

The unsatisfactory outcomes with double sided carbon tape directed us to develop a different sample preparation methodology, specifically sample supports having different elemental composition from Al or Si, so that sample particles and related materials that contain Si and/or Al could be characterized using electron beam techniques with less background interference. Other considerations included minimization of cross-contamination and elemental overlap between the sample and its supporting substrate, and the substrate should be readily cleaned between samples to enable reuse across different sample types for savings in terms of time, cost, and materials to minimize waste. Lastly, a conductive holder ensures that the substrate does not impact the determination of the elemental composition of nanoscale and larger zeolite-based materials while also enabling electron conduction during SEM and EDS analyses.

Polished copper (Cu) stubs provide a conductive, planar substrate that satisfies the criteria mentioned above. However, zeolite particles were observed to irreversibly adhere to the Cu/CuO_x film on the surfaces of the stub that develop spontaneously in air over time, due to the high surface energy of these polished Cu substrates. Washing, sonication, and repolishing did not remove the particles. With the aim of reusing the Cu stubs, an additional process was required to minimize repolishing of the stub between samples and to extend the usable lifetime of these sample supports.

A polymer film applied to the Cu stub would bypass the adhesive energy of the Cu stub, and, ideally, would offer a reversible interaction between the zeolite materials and the substrate. Cast polymer films lower the surface energy of metal substrates and can be used to mitigate the adhesive interactions between various samples and metal substrates.[20,21] Any film created would also need to be sufficiently thin to avoid charge build-up on the sample materials during SEM and EDS analyses. A method was developed here to spin coat a polymer film onto polished Cu stubs through a process that enabled tuning of both the thickness and composition of these films. A film thickness of ~1 μm was empirically identified as a starting point based on prior reports for enabling SEM analyses of materials supported on top of such films while reducing background interferences.[20,22,23] Films cast from solutions containing suspensions of polymers tend to be less robust as they can be displaced or otherwise removed from the substrate by the solvents conveniently used in drop-casting of zeolite materials.[24] However, polymers cast as a thin film onto the substrate and then cross-linked can exhibit an increased stability when exposed to a wide variety of solvents, while also retaining sufficient conductivity to minimize sample charging during SEM and EDS analyses.[25,26] We hypothesized that a polished Cu stub coated with an experimentally generated thin film of a cross-linked polymer could be used as a reusable substrate for enabling the characterization of non-conductive particles (e.g., silicates, ceramics), which was demonstrated through the analysis of zeolite-based particles and other aluminosilicate materials.

2. Experimental Section

2.1 Overview of the Fabrication Process to Prepare the SU-8 Coated Cu Stubs

The step-by-step process of preparing the Cu stubs is depicted in the summary in Figure 1. The total preparation time for this sequence is ~2 h per polymer coated Cu stub. The Cu stubs enabled

direct insertion, without modification, into standard sample holders available for analysis by SEM and EDS techniques. The polymer coated Cu stubs, with and without zeolite particles were able to be analyzed by commercial scanning electron beam instruments. There was no other modification or additional conductive coating (e.g., C or Ir film) applied.

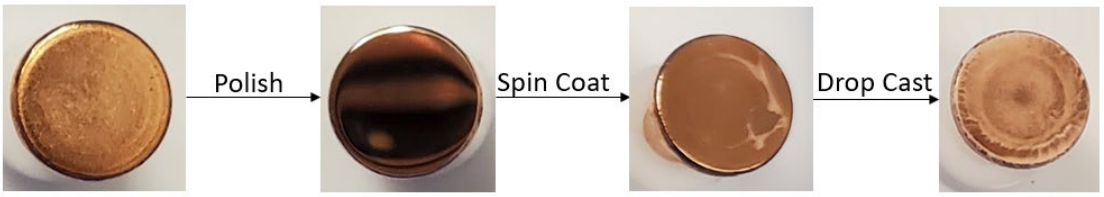

Figure 1. Images depicting select steps in the process of preparing a polished copper (Cu) stub followed by spin coating and ultraviolet (UV) irradiation to create a thin film of cross-linked SU-8 polymer onto which zeolite particles are then deposited through drop casting.

2.2 Reagents and Standards

The SU-8 2002 (photoresist), SU-8 thinner, and SU-8 developer were purchased from Micro-Chem Laboratories Inc. (Seattle, WA, U.S.A.) to coat the copper (Cu) stubs supplied by Ted Pella Inc. (Copper Mini Pin Stub for ZEISS/LEO with a 6.25 mm pin length, and a head with a 6.6 mm diameter and 1.2 mm thickness; Redding, California, U.S.A.). Other polymers evaluated in this study included polystyrene (M_w ~280k; Aldrich Chemical Company, Inc., Milwaukee, Wisconsin, U.S.A.), poly(methyl methacrylate) (M_w ~15k; Sigma-Aldrich, Inc., St. Louis, Missouri, U.S.A.), and poly(sodium 4-styrene-sulfonate) (M_w ~70k; Sigma-Aldrich, Inc., St. Louis, Missouri, U.S.A.). Solutions of these polymers were created in toluene (≥99.5% CMOS grade; Avantor Performance Materials, Inc., Center Valley, Pennsylvania, U.S.A.), which were used to prepare a series of thin polymer films. Reagent grade isopropanol (70% in H_2O), used for dispersing the zeolite particles, was purchased from Sigma-Aldrich (Oakville, Ontario, Canada). Ultra-high purity (UHP) water, having resistivity of 18.2 MΩ·cm was obtained from a Barnstead MicroPure

System, was used for removing zeolite particles from the polymer coated Cu stubs after completing electron beam characterization of each set of particles. Three different zeolite standards, ammonium ZSM-5 type samples, were purchased from ThermoFisher Scientific (Waltham, Massachusetts, U.S.A). The manufacturer reported SiO_2:Al_2O_3 mole ratios of these standards, which are converted into Si:Al mole ratios as presented in Table 1 for ease of comparison to the results of the analyses reported herein.

Table 1. Si:Al Molar Ratio of the ZSM-5 Zeolite Standards

Name of Zeolite	Si:Al Molar Ratio Reported in the COA[†]
ZSM-5-11	11.1:1
ZSM-5-45	45:1
ZSM-5-161	161:1

[†]Certificate of Analysis (COA)

2.3 Polishing of the Cu Stubs

Manual polishing was used to reduce the nominal surface roughness to improve the differentiation of zeolite particles from the support. Diamond film lapping sheets were used to complete this task [Diamond Lapping Film Sheets with 30, 6, and 3 μm grit were purchased from Thorlabs (Newton, New Jersey, U.S.A.)]. A custom plastic holder was used to grip the Cu stubs while the stubs were manually moved in a "figure eight" pattern upon the polishing sheets. This polishing process was performed using each of the sheets in decreasing grit size until the visual appearance of the stub (e.g., color and reflection) was unchanging. Between each polishing step, the Cu stubs were cleaned by ultrasonication in UHP water for 2 min (Ultrasonic Cleaner, BRANSONIC serial number RMC040844828F, 100 Watts), then rinsed with an excess of UHP water, followed by drying under a stream of compressed, filtered nitrogen (N_2) gas to remove polishing residue. Additional polishing steps using a series of five diamond pastes of a sequentially

smaller particle dimension, placed on Buehler Nylon pads (Buehler; Lake Bluff, IL, U.S.A.) further smoothed the surface of the Cu stubs until a mirror finish was obtained. Scratches visible only upon inspection with an optical microscope were present yet were assumed to not be significant factors in precluding qualitative and quantitative interpretation of the data. The particle dimensions in the diamond pastes were 1 μm and 0.5 μm (Hyprez five star paste) supplied by Engis Corporation (Wheeling, IL, U.S.A.) and 0.25 μm, 0.1 μm, and 0.05 μm (Polycrystalline paste) supplied by Allied High Tech Products, Inc. (Compton, CA, U.S.A.). The Cu stubs were polished against the series of polishing pads, each containing a unique diamond paste, changing the pads in sequence of descending particle size. During each polish step, the Cu stubs were held using a custom plastic holder and gentle pressure was applied by hand while moving the stub in a "figure eight" pattern for 5 min on each pad. Polished stubs were rinsed with UHP water between each of the polishing steps along with cleaning for 1 min by immersion in fresh UHP water in a sonicator. This rinsing process was adopted to avoid cross contamination between polishing pastes.

2.4 Spin Coating of a Polymer Coating

A semi-permanent polymer coating was created by applying and then cross-linking a film of SU-8 on the Cu stub. This polymer was selected as a target material to formulate a coating on the Cu stubs for the relative stability of the SU-8 polymer under the focused electron beam of a SEM and for its ability to be cross-linked for improved durability of the polymer film.[26] The SU-8 monomer consists of an epoxy-based resin along with a photoinitiator suspended in an organic solvent (e.g., cyclopentanone or gamma-butyrolactone). Triaryl sulfonium hexafluoroantimonate salts that serve as the photoinitiator release a Lewis acid upon exposure to a sufficient dose of ultraviolet (UV) light. This Lewis acid serves to catalyze cross-linkage of the epoxide functional groups on the suspended SU-8 monomers. Both a pre- and post-UV-exposure bake are also

normally included in the formation of an SU-8 polymer film.[27] A pre-UV-exposure bake serves to remove excess solvent, while a post-UV-exposure bake serves to increase the rate of cross-linkage of the SU-8 monomers. A solution of SU-8 2002 monomers was diluted 10x with an SU-8 thinner (a 20x dilution was also evaluated herein). Approximately 15 μL of the diluted solution was applied using an adjustable pipettor to a stationary Cu stub. A spin coater (Brewer Science, Model 100, serial number 992040914652) was used for controlling the ramp rate, spin speed, and the duration of each step in the spin coating process. The spin coater was programmed to increase its speed at 500 rpm/s until achieving 2000 rpm, which was maintained for 90 s, and then the speed decreased to 0 rpm. After spin coating the SU-8 2002 suspension of SU-8 monomers, the Cu stub was then inserted into a pre-drilled hole on an Al plate, held at 95 °C, for a 90 s pre-UV-exposure bake of the SU-8 film.

A microscope with a built-in mercury vapor UV lamp was used to trigger the polymerization process for cross-linking of the spin coated SU-8 films (further details of the microscope are outlined in section 2.6.1). The SU-8 film on the Cu stub was exposed to UV light for 20 s (UV A: 20.3 mW/cm^2, UV B: 80.5 mW/cm^2) with the microscope set to bright-field (BF) mode and a 2.5x magnification. A red-light filter on the microscope was used to inspect the SU-8 film on the Cu stub both before and after the UV exposure for uniformity of the polymer film. The polymer coated Cu stub was again placed back onto the Al plate (T = 95 °C) for 3 min to perform a post exposure bake, which is known to promote further cross-linking within polymer thin films. The cross-linked film was subsequently rinsed with SU-8 developer solution (~3 to 5 mL) to remove polymer that had not cross-linked. The developer was dispensed onto the polymer coating on the Cu stub using a glass Pasteur pipette in a repetitive manner for a period of 1 min, and then the film was further rinsed with isopropanol by immersing it in ~5 mL for 10 s. A stream of compressed, filtered N_2

gas was then used to dry the film. This process achieved a cross-linked polymer coating with a thickness of ~1 μm on the polished Cu stubs as determined by SEM analyses of cross-sections prepared by mechanically removing a portion of these films. Prior to use, a qualitative assessment of each polymer coating was conducted visually to ensure that the entire surface of the Cu stub was covered and reflected light uniformly. A set of polymer-coated Cu stubs were prepared such that each zeolite standard (Table 1) was placed on a different polymer coated stub.

2.5 Application of Zeolite to the Cu Stubs and Cleaning Procedure for Reuse of Stubs

The zeolite materials were applied by drop-casting from a suspension in isopropanol onto the SU-8 coated Cu stubs. The protocol for sample preparation for SEM and EDS analyses involved dispersing 0.5 mg of each zeolite particle standard (Table 1) in 2 mL isopropanol. For each solution, 15 μL aliquots were pipetted onto the polymer coated Cu stubs. The isopropanol was evaporated prior to any characterization. After analysis, the zeolite materials were removed from the Cu stubs for re-use of the substrate. The zeolite materials were removed by simply submersing each stub in a beaker containing 5 mL of UHP water, and then placing this beaker into an ultrasonicator for 1 min. The stubs were subsequently rinsed with an excess of UHP water and dried under a stream of compressed, filtered N_2 gas.

2.6 Instrumentation

2.6.1 Optical Microscopy Modes

An optical microscope (Zeiss Axio Imager.M1m) was used for imaging the Cu stubs before and after polishing, and throughout the polymer spin coating process to monitor the uniformity of the coating on the Cu stub. Various magnifications (e.g., 25x, 50x, 200x) were used to image these substrates. Imaging modes used to visualize the surfaces included dark-field (DF), bright-field

(BF), differential interference contrast (DIC), and circular-DIC (C-DIC). The C-DIC and DIC modes provided feedback on variations in the film topography across the surface of each stub.

2.6.2 SEM Parameters

A SEM (FEI/Aspex Explorer) was used in the analysis of the zeolite particles and for further analysis of the topography of the unpolished and polished Cu stubs. This instrument was equipped with an oil-free pumping system with a high vacuum imaging mode that enabled use of a tungsten (W) filament emission source and either a secondary electron detector (SED) or back scattered electron detector (BSED). The SED was operated at a 25 kV accelerating voltage applied to the electron beam. An OmegaMax SDD EDS detector was used to analyze the elemental composition, reported as relative weight percentages, of the samples. The EDS settings for these analyses included integration of the measured signal over a 2 min period that enabled quantitative determination of elemental weight percentages for Si and Al for each location imaged. An FEI Helios SEM NanoLab 650 SEM/FIB dual beam system was also used for high resolution imaging of the Cu stub surface pre- and post-polishing. This imaging was conducted in Secondary Electron mode at an accelerating voltage of 5 kV and a beam current of 0.1 nA.

2.6.3 STEM Parameters

A scanning transmission electron microscope (STEM) (FEI Tecnai Osiris) operated with an accelerating potential of 200 kV applied to the focused electron beam was used as a complementary analysis of the zeolite particles. This instrument had an oil-free pumping system with an X-FEG Schottky field emitter that provides a high emission of electrons. This instrument was also equipped with an Analytical TWIN objective lens integrated with a Super-X EDS detector system that is based on Silicon Drift Detector technology. Dimensions of the zeolite particles were determined via TEM imaging techniques and maps of the elemental compositions of these particles

were obtained via STEM techniques. Three to five separate particles were analyzed for each sample by STEM techniques to have results from several particles to compare to the SEM analyses.

The protocol for sample preparation for STEM involved dispersing 0.5 mg of each zeolite particle standard (Table 1) in 2 mL isopropanol. For each solution, 4 μL aliquots were pipetted onto carbon coated Formvar 200 mesh copper TEM grids (purchased from Ted Pella Inc., Redding, California, U.S.A.). The grids were handled using gold-plated TEM tweezers. These grids were subsequently dried in a vacuum desiccator (~230 Torr) for 12 h before analysis.

3. Results and Discussion

3.1 Analyses of Zeolite Particles Supported on Carbon Tape

Double-sided C tape was applied to cover the entire surface of the Al stub exposed to the electron beam. In assessing the C tape as a potential substrate, various areas of a section of tape with visually different morphologies were analyzed using EDS. For each region, the EDS signal was integrated over a singular point as well as over a larger area of the carbon tape. To improve counting statistics for a determination of the weight percentage of an element in a sample, the integration time was held at 2 min for both the point analyses and the selected larger areas (e.g., Figures S1 to S4). The signals for the selected different areas of the C tape yielded variations in the weight percentages (wt%) of Si and Al, and attributable in part to observable inhomogeneity in tape thickness. Different regions that were each loaded with a sample of zeolite particles were also observed to generate large variation in the wt% of Si and Al, which supported the assumption that the tape itself contained silica and alumina contamination.[28,29] A lack of consistent and reproducible results, as described above, indicated that another method was required for supporting zeolite particles to measure their elemental composition using EDS techniques more reliably.

3.2 Screening of Polymer Coatings on Cu Stubs: Optical Microscopy Analyses

In turning attention from strategies to suppress signals from the underlying sample support, stubs made of Cu were investigated. In the initial experiments with Cu stubs, it was observed that

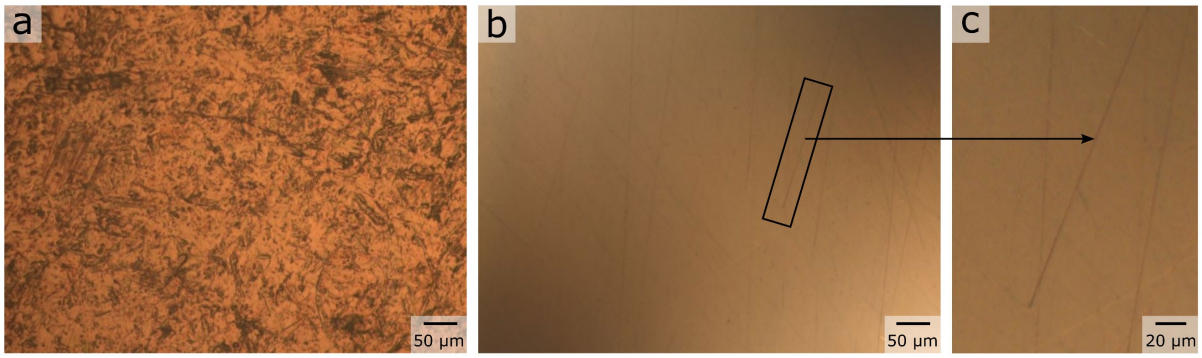

Figure 2. Optical microscopy images of (a) the Cu stub before polishing, (b) the Cu stub after polishing, and (c) a magnified view of a scratch on the surfaces of a Cu stub. All images [(a), (b), (c)] were obtained at a magnification of 200x while using the brightfield (BF) imaging mode.

polishing to create a smooth planar substrate was needed because the initial topography on each of the stubs had visible variations that were significantly greater than the dimensions of the zeolite particles. Representative images of the copper stubs, acquired using an optical microscope before and after polishing, are in Figure 2. The polishing step resulted in a significant change in the topography and surface roughness of the stubs. However, scratches observable at magnification remained on the polished surfaces of the Cu stub [Figure 2(c)]. The extent of the scratches on the copper stubs was assessed by optical microscopy using BF and DF imaging modes, which guided further refinements to the steps used for processing the Cu stubs (Figure S5). Additional analyses of the unpolished and polished Cu stubs were pursued by SEM analyses, which confirmed the coarse topography of the as-received stubs versus the comparative smoothness after polishing (Figures S6 and S7). Unfortunately, removal of zeolite samples from the Cu stub required extensive, time intensive polishing.

In further exploration of the Cu stubs as supports, polymer films generated by spin coating were evaluated as a reusable substrate for the analysis and subsequent removal of the zeolite particles. Using a series of polished Cu stubs, various polymer solutions were spin cast onto a series of individual stubs. Two types of polymers were evaluated for this purpose—both non-cross-linked polymer films that were used as cast onto the Cu stubs, and polymer films similarly generated that were subsequently cross-linked on the Cu stubs. Each film was assessed for its uniformity, its stability during removal of zeolite particles, and its reuse in subsequent analysis of additional zeolite particles. The polymer coatings were first evaluated for their ability to create a smooth surface atop the polished Cu stubs, and to remain unchanged under interrogation with the focused electron beam of the SEM across different samples loaded onto the stub. Past studies have identified a series of polymers that can form uniform coatings on polished Si wafers, which have been shown to produce relatively smooth topographies, as well as to be sufficiently electrically conductive for SEM imaging.[20,30-33] In addition, in this work, it was noted that zeolite particles when deposited on a polymer film were readily observable and distinct from topological features remaining on a stub after polishing.

Non-cross-linked polymers were evaluated for their use as protective coatings on the Cu stubs while retaining sufficient conductivity during the SEM analysis of the zeolite particles cast upon their surfaces. The solutions of polymers that were evaluated for coating the Cu stubs included a 2% (wt/v) polystyrene in toluene, 2% (wt/v) poly (sodium-4-styrenesulfonate) in water, and 2% (wt/v) poly (methyl methacrylate) in toluene. The selection of solvents and the weight percentage of polymers used to prepare these solutions were optimized based on their ability to form thin, uniform films with an expected thickness of <1 μm on polished Si wafers. These polymer solutions were subsequently applied to a series of polished Cu stubs, then spin coated as outlined in Section

2.4, except that for these solutions a ramp speed of 100 rpm/s was used to reach a target speed of 2000 rpm that was maintained for 30 s. The polymer coated Cu stubs were then placed into reservoirs on an Al plate that had been placed on a hot plate at 180 °C and held at this temperature for 10 min (the higher temperature than outlined in Section 2.4 was designed to remove residual toluene from these non-cross-linked polymer films). The stubs were next transferred to another Al plate to cool to room temperature before observing them under the optical microscope (e.g., Figures S8 to S10).

When characterizing the coatings cast from solutions of polymers as observed by optical microscopy, the uniformity of each coating was assessed by the regularity of its appearance under BF, DF, and DIC imaging. The use of DIC imaging enabled an assessment of variations in height (Figure S5) of <50 nm across the samples.[34] In representative images (Figures S8 to S10), these trial studies produced relatively uneven films having surface irregularity and roughness on the Cu stubs. These features suggested the formation of domains within the cast films attributed to variation in wetting of the stubs by the solvents and polymer and hence precipitation, and residual roughness of the polished Cu stub. On these films, zeolite particles with average dimensions of ~1.8 μm were difficult to differentiate from the coating. Also, rinsing of these non-cross-linked polymer coatings in a solvent with manual agitation did not remove the zeolite particles from the polymer coated substrates. Sonication of the polymer coated Cu stubs conducted in UHP water for 1 min removed the zeolite particles from the polymer coatings as confirmed at higher magnifications, but that sonication step also effected partial removal of the film. These results collectively indicated that coatings prepared from non-cross-linked polymer films were not sufficiently durable to withstand the necessary cleaning step using ultrasonication to remove the zeolite particles for reuse of these stubs.

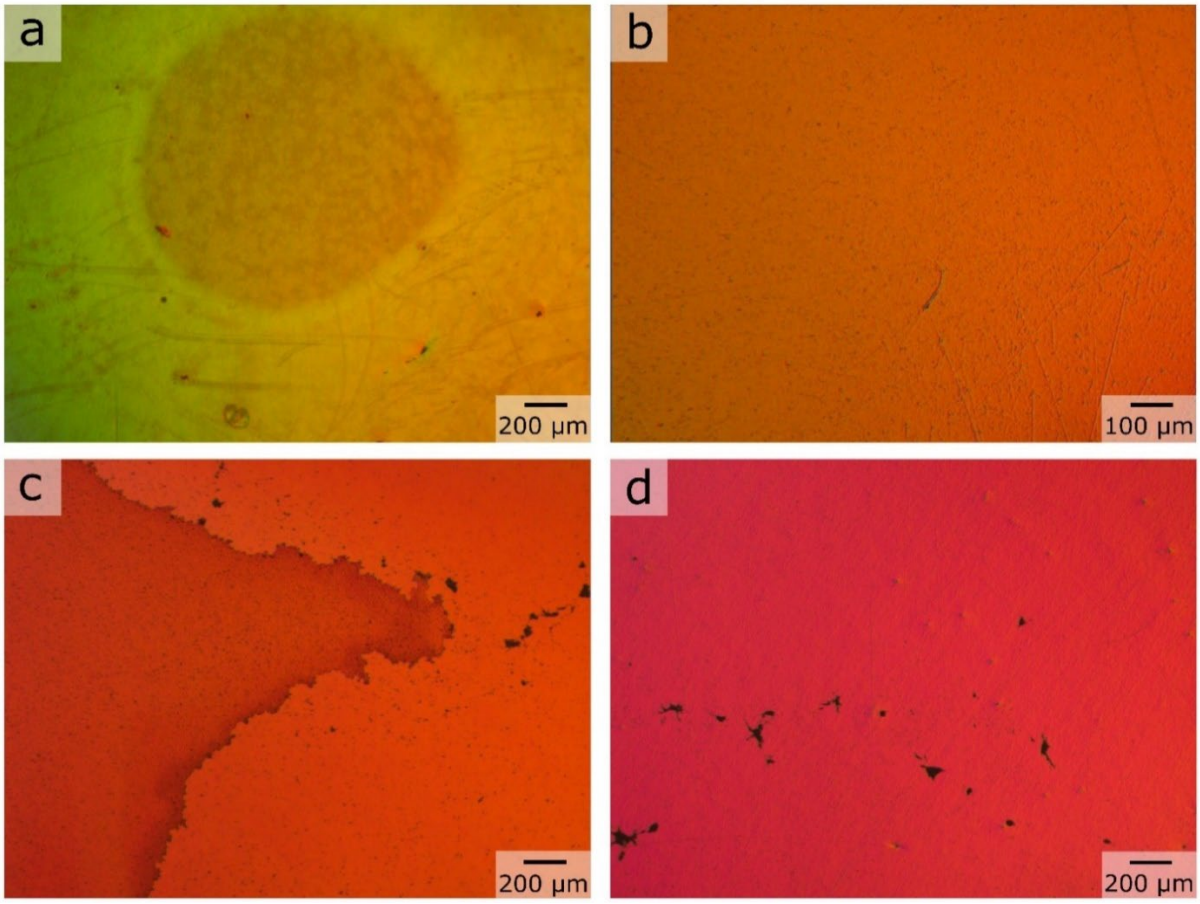

Figure 3. Optical microscopy images obtained using a circular differential interference contrast (C-DIC) imaging mode of (a) the Cu stub after coating with a 20x diluted SU-8 2002 solution; (b) the Cu stub after coating with a 10x diluted SU-8 2002 solution; (c) an example of a distribution of zeolite particles exhibiting the "coffee-ring effect" on a thinner film of SU-8 polymer; and (d) zeolite particles more evenly dispersed upon a thicker SU-8 polymer coating.

A series of cross-linked polymer films were prepared from an SU-8 monomer, which is a commercially available, chemically and physically durable negative photoresist. Solutions of SU-8 monomer were cast onto the Cu stubs, which were cross-linked using UV irradiation followed by a thermal treatment. Two different solutions prepared from 10x and 20x dilutions of a commercial source of SU-8 monomers, were selected for their ease of coating a variety of

substrates of varying roughness. These polymer solutions were applied to Cu stubs, spin coated, and cross-linked following UV irradiation and a thermal treatment as outlined in Section 2.4. The 20x diluted suspension, targeting a final film thickness of <1 μm if applied to an atomically smooth substrate,[26] was observed by optical microscopy to not create a uniform film. In comparison, the 10x diluted suspension appeared to create a more uniform film as assessed using optical microscopy (Figure 3).

Zeolite particles dispersed in isopropanol were drop cast onto the polymer coatings. Zeolite particles deposited onto the film generated using the 20x dilution of the SU-8 monomer were observed around the edge of the stub, likely due to the "coffee–ring" effect.[35-39] This effect occurs when capillary flow causes suspended solids to move towards the edges of the substrate where local solvent evaporation causes zeolite particles to accumulate.[35,36]

If the solvent fraction of a suspension of SU-8 monomers is not well matched to the surface it is being applied to, as in the case of the 20x diluted solution of SU-8 monomers, irregular wetting of the polished Cu substrate can occur during spin coating. As mentioned previously, the polished Cu stub has texture that was not removed by polishing (Figure S7), and that can contribute to the formation of a coating having an irregular texture, especially if the cast film is of an insufficient thickness to cover the remaining features on the Cu stub. As a result, the isopropanol solution containing the zeolite particles cast upon a polymer substrate having a non-uniform texture and potentially regions of exposed Cu stub, may have led to differential isopropanol evaporation rates at different areas of the stub, leading to an inhomogeneous distribution of zeolite particles.[37] Conversely, when using the thicker polymer films prepared from the 10x dilution of SU-8 monomers, the zeolite particles deposited in a more even distribution across the Cu stub. This suggests the spin coating of the 10x diluted solution of SU-8 monomers had significantly less

371 irregularity in its coverage of the Cu stub relative to that for the 20x diluted solution of SU-8
372 monomers. Prior work has suggested that an even distribution of particles across a substrate is
373 largely the result of a uniform evaporation of the solvent across a surface.[35-39] These observations
374 suggested the 10x dilution of SU-8 monomers was preferable. Thus, the 10x dilution of SU-8
375 monomer solution was selected to prepare the SU-8 polymer coatings for further studies.
376

3.3 Analysis of the Polymer Coated Cu Stubs and Zeolite Particles by SEM and EDS

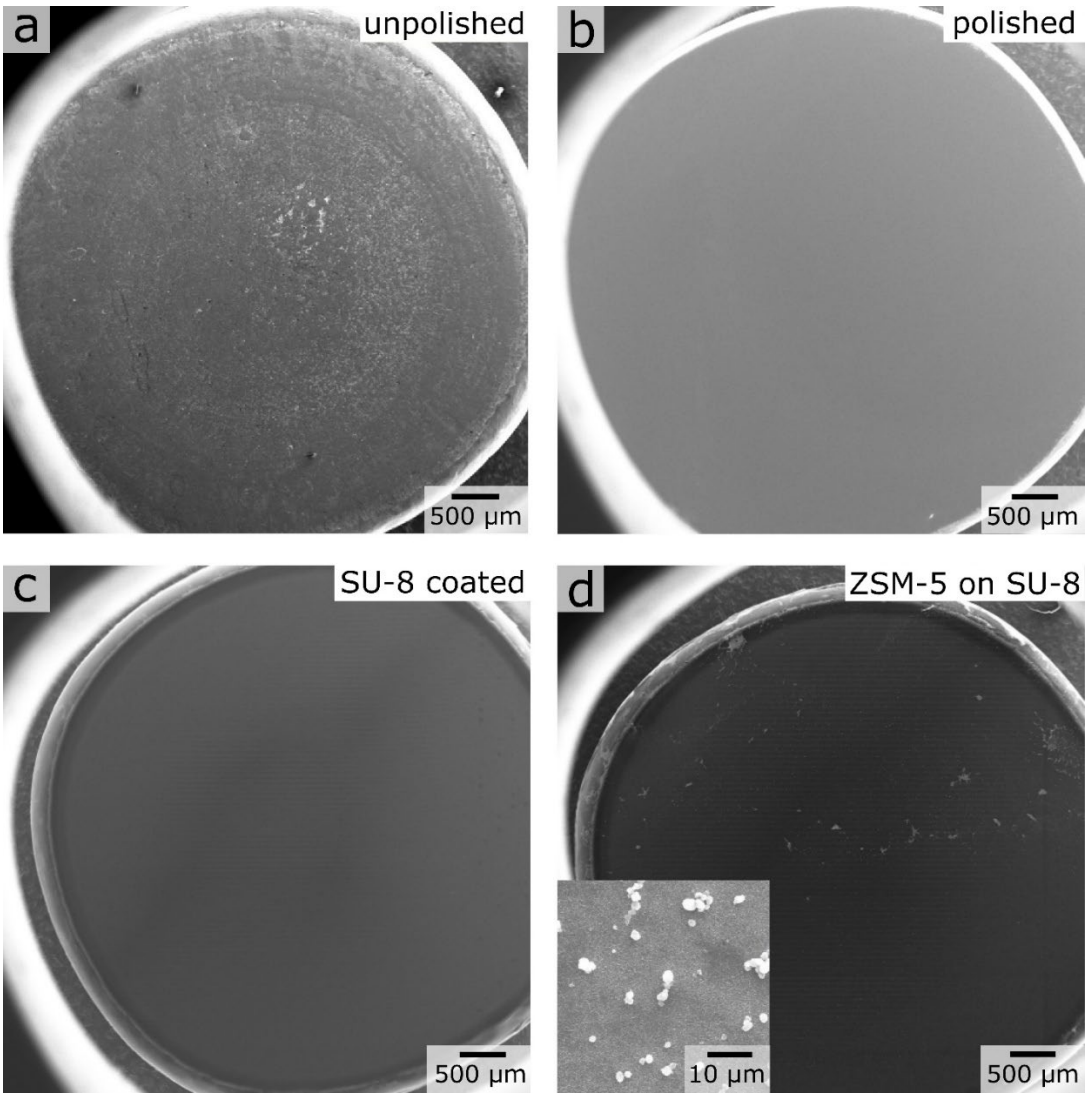

Figure 4. Representative scanning electron microscopy (SEM) images of: (a) as-purchased, unpolished Cu stub; (b) polished Cu stub; (c) Cu stub coated with a film of SU-8 based polymer after cross-linking by ultraviolet (UV) irradiation; and (d) ZSM-5-161 particles deposited on a polished Cu stub coated with a film of SU-8 based polymer (inset shows a magnified view of ZSM-5-161 particles).

The Cu stubs were analyzed by SEM techniques before and after the polishing process, after coating these substrates with a cross-linked SU-8 polymer film, and after applying the zeolite

382 particles (Figure 4). Polishing resulted in a significantly smoother surface with only minor surface
383 defects [Figures 4(b) and S7]. Some of the observed surface defects were determined *via* EDS to
384 be carbon particles that possibly remained on the substrates because of the polishing process (e.g.,
385 diamond paste residue) and, therefore, would not interfere with the elemental analysis of the zeolite
386 materials. Figure 4(c) shows a representative SEM image of a Cu stub coated with a polymer film.

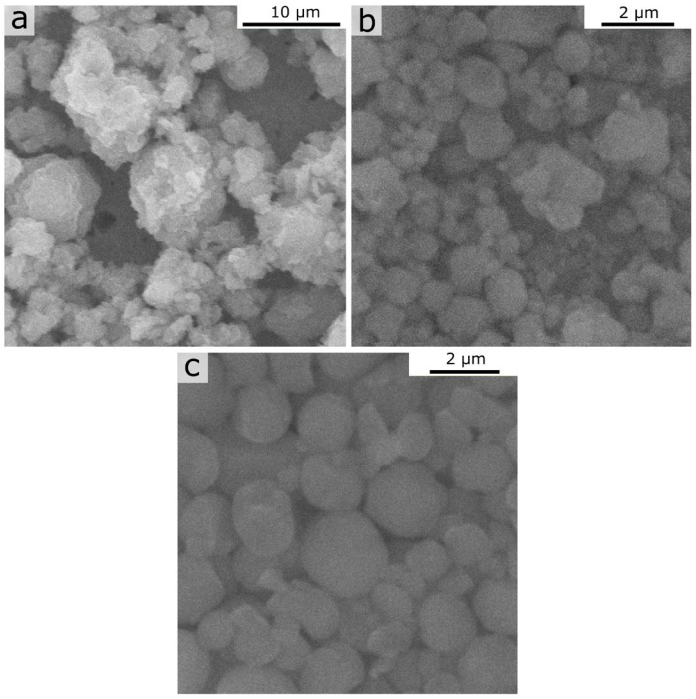

Figure 5. A series of SEM images obtained using a secondary electron detector (SED) during the analysis of ZSM-5 zeolite particles deposited onto a film of cross-linked SU-8 polymer supported on polished Cu stubs. These particles were reported to contain Si:Al in nominal mole ratios of (a) 11:1, (b) 45:1, and (c) 161:1.

387 There were a couple of regions of non-uniformity in the polymer coating that were centered on
388 carbon particles that were present on the polished surfaces (e.g., residue resulting from the
389 polishing step). As mentioned in Section 3.2, when zeolite particles dispersed in isopropanol were
390 drop-cast onto the polymer coated stubs, the particles were evenly dispersed across the stub.
391 Despite observable variations in the thickness of the polymer coating, the wetting by the solution

of zeolite particles was dictated by the properties of the SU-8 based polymer. After solvent evaporation, the particles adhered to the polymer coating, as evidenced by subsequent SEM and EDS results for the three zeolite particle standards. No indication of charging was observed in these samples supported upon the SU-8 coatings. Representative images of each of the standard zeolite particles, heavily loaded, on the polymer coatings are presented in Figure 5.

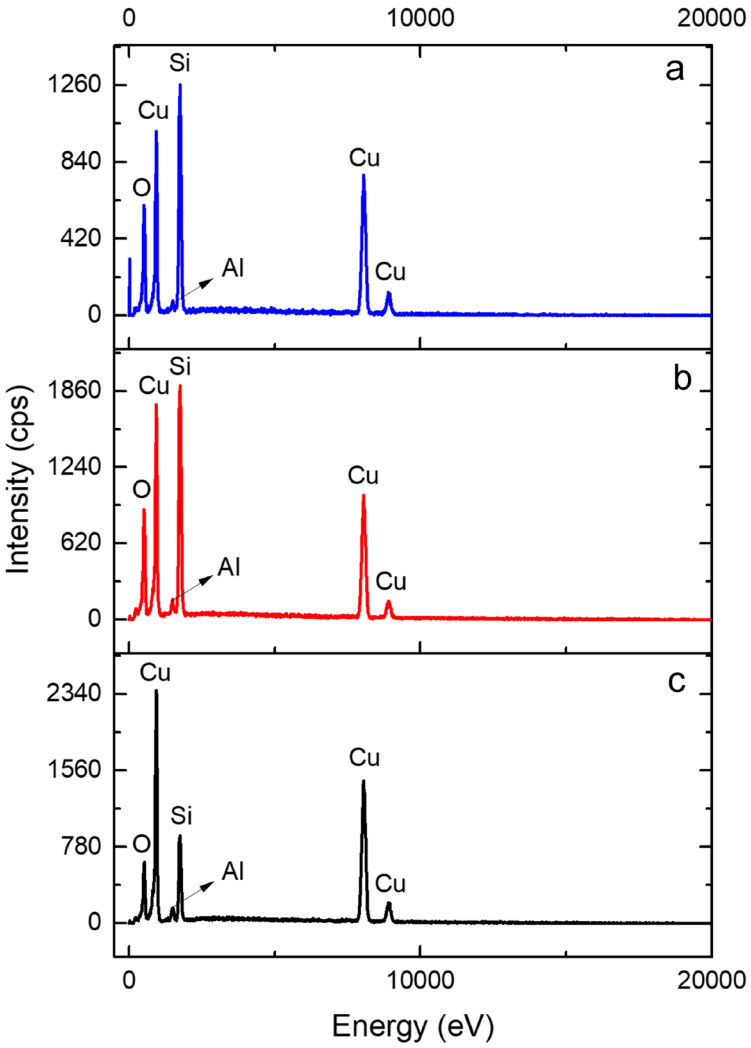

Figure 6. Representative EDS spectra obtained by SEM techniques for standard ZSM-5 zeolite particles with reported Si:Al mole ratios of (a) 161:1, (b) 45:1, and (c) 11:1.

Zeolite particles at several different locations of the zeolite-loaded stub were analyzed to understand variations in the inter-particle composition, and what contributions from impurities in

399 the sample or from the sample support (e.g., Cu stub and/or the polymer coating) cause
400 interferences. The EDS spectra of the polymer coated Cu stubs revealed that Cu signatures were
401 observed even with the cross-linked polymer coating (Figure 6). The Cu signals were not included
402 in the calculations to determine the Si:Al mole ratio for each of the particles. The wt% used to
403 calculate the at% of the various elements in each of the zeolite particle standards was obtained
404 through the software for the SEM by integrating the respective peaks in the corresponding EDS
405 spectra. In contrast, the peak area ratios calculated for each type of zeolite standard after removing
406 the Bremsstrahlung and other background contribution appeared to give a more linear response
407 (Table 2). The EDS data shows that the relative at% of O remained relatively constant between
408 the samples. The at% of Cu varied between the samples, likely due to changes in the loading and
409 size of the zeolite particles being analyzed (e.g., influencing the relative attenuation of the incident
410 electron beam). Incorporation of a zeolite particle size factor in measurements of the Cu signals
411 could be investigated in the future for potential use as an internal standard. Furthermore, since the
412 Cu stub and SU-8 based polymer coating each contribute to the at% of O, in addition to the
413 contributions from the zeolite particles, it was determined that O could not be quantified.
414 Quantitative analysis was restricted to the Al and Si abundances in the samples.

415 The Si:Al molar ratios for each of the zeolite particle standards as determined by two
416 separate methods are reported in Table 2. The Al at%, as calculated from the wt% reported by the
417 EDS software, decreased relative to the at% of Si in accordance with the data reported by the
418 supplier for this series of ZSM-5 zeolite standards. The Si:Al molar ratios determined from these
419 at% values were, however, significantly lower than the molar ratios reported for each standard
420 (Table 2). The trend observed for the Si:Al ratios derived from the at% of both Si and Al was also
421 non-linear. A linear correlation was, however, found when manually integrating the peak areas for

both the Al and Si species and comparing their peak area ratios to the reported mole ratios for these three ZSM-5 zeolite standards (Figure S11). A linear correlation is expected for EDS analyses performed by SEM techniques. It should, however, be noted that the specific correlation derived herein will likely vary with instrument conditions (e.g., changes to accelerating potential of incident electrons and detector specific sensitivity factors). It is recommended that another form of validation be used to confirm the trends observed within and between each of the distinct standard samples (e.g., analysis by X-ray photoelectron spectroscopy). The observations from the analysis of the zeolite standards did indicate that SEM and EDS results for samples supported on polymer coated Cu stubs could be used as a quantitative tool to determine the elements that are present within these particles without any background interference from Si or Al within the sample support.

Table 2. Measured Atomic Percentages and Peak Area Ratios for the Standard Zeolite Particles

Reported Si:Al Ratio	Si (at%)	Al (at%)	Si:Al from EDS Atomic % Ratio†	Si:Al from EDS Peak Area Ratio‡
11.1:1	12.7 – 14.4	1.5 – 1.8	8:1 to 8.5:1	9.7:1
45:1	7.4 – 8.1	0.33 – 0.38	21:1 to 22:1	14:1 to 15:1
161:1	8.9 – 9.6	0.22 – 0.29	33:1 to 40:1	26:1 to 27:1

† Uncorrected atomic percents as determined from weight percentages reported by EDS analyses software.

‡ Peak areas determined after background subtraction and a manual integration of both the Si Kα and Al Kα peaks. This peak area ratio exhibits a linear correlation to the reported mole ratios (Figure S11).

3.4 Analysis of Zeolite Particles by TEM Techniques

Isolated particles for each zeolite standard were imaged using TEM techniques. These analyses indicated the presence of fewer particles with rounded edges in the 11:1 standard, and a gradual increase in the presence of particles with rounded edges in the 45:1 to the 161:1 ZSM-5 zeolite standards (Figure 7).[1] The morphology of the particles as observed by TEM imaging is in general agreement with the data provided using SEM imaging of the samples. This change in morphology

444 is consistent with a higher Si content in the zeolite materials because of its influence on the atomic
445 structure of these mesoporous materials.[1]

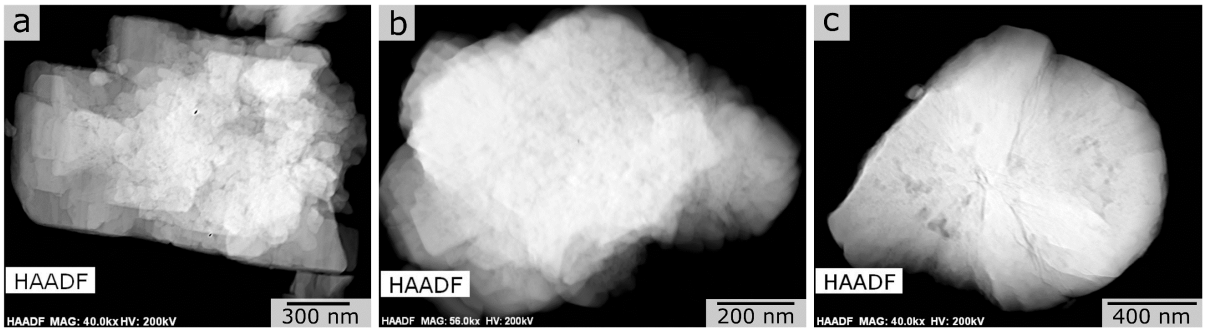

Figure 7. Scanning transmission electron microscopy (STEM) based high-angle annular dark field (HAADF) images of standard zeolite particles reported to contain Si:Al ratios of (a) 11:1, (b) 45:1, and (c) 161:1.

446 Lastly, the elemental distributions across individual particles, plotted as heat maps, were
447 measured for the particle standards by EDS using TEM techniques to further characterize the
448 relative distribution and abundance of Si, Al, and O within the standards. For the particle depicted
449 in Figure 7c, the heat maps depicting spatial variations in the elemental compositions of the 161:1
450 standard are presented in Figure 8. This analysis also provided further confirmation that Si was the
451 major component in the ZSM-5 zeolites in comparison to Al, as expected for the ZSM-5
452 zeolite.[40,41] Similar heat maps obtained through the EDS analysis using TEM techniques for the
453 45:1 and 11:1 ZSM-5 zeolite standards (Figure 7a and 7b, respectively) are provided in Figures
454 S12 and S13, respectively.
455

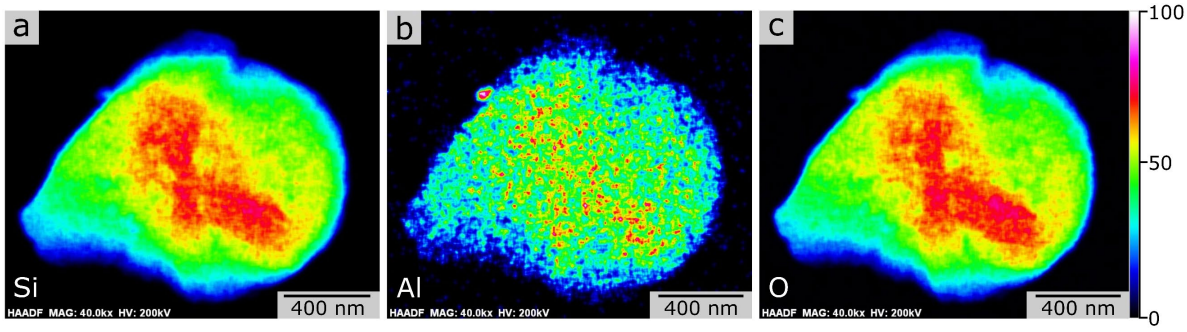

Figure 8. Elemental distributions depicted as heat maps for (a) Si, (b) Al, and (c) O as obtained by TEM based EDS analyses of a 161:1 (Si:Al) standard zeolite particle. The colors in these maps indicate the relative abundance of the elements with higher concentrations indicated by red and lower concentrations by blue as indicated in the vertical scale bar. Zeolite particles were drop cast onto a copper TEM grid.

3.5 Analysis of the Reusability of the Polymer Coated Cu Stubs

It was found that the SU-8 polymer coated Cu stubs could be reused after removing the previous zeolite sample using sonication in UHP water for 1 min. This process of removing the particles could, however, impact the quality of the polymer coating because of the mechanical agitation and heating induced by cavitation during the sonication period.[42] In this study, it was observed that the polymer coated Cu stub could be reused for the analysis of up to approximately ten different samples without a negative impact on the coating from the sonication process. Further reuse the SU-8 polymer coated Cu stub resulted in observably increased adhesion of particles at the perimeter of the polymer coated Cu stub following the drop-casting process, and simultaneously, decreased integrity of the film proximal to the perimeter of the stub. The latter was attributed to the sonication process (Figure 9). In support of those observations, the relative intensity of the Cu signal as observed by EDS analysis started to rapidly increase and the film quality as observed by SEM imaging decreased with each re-use of the cross-linked SU-8 polymer

coated stub. Figure 9 demonstrates the copper signal observed by EDS for an uncoated copper stub, a copper stub freshly coated with SU-8, and the same stub after different stages of use in the analysis of zeolite particles. The EDS spectra in this figure shows that the Cu signal increases with repeated use of the polymer coated Cu stub using the sonication method to remove the zeolite particles. The results also indicated that the elemental composition of the zeolite particles could no longer be precisely determined with repeated exposure of the cross-linked SU-8 coating after approximately ten sonication cleaning events because of incomplete removal of zeolites from the prior trial, and thus, sample to sample cross-contamination taking place. It was, therefore, determined herein that <10 uses were an empirical maximum number of times the coating generated using the SU-8 based polymer should be reused, both with respect to irreversible adherence and inaccuracy of the elemental analysis of the zeolite particles. When replicating this work, the quality of these polymer coatings should be monitored by SEM to ensure minimal Cu is exposed since it requires more extensive cleaning (e.g., polishing) to ensure prior samples are removed. The procedures reported herein significantly improve sample to sample characterization using the same stub, with an overall decrease in the time needed for sample preparation when considered across multiple samples. Further improvements in the resilience of the polymer coating could be possible through further optimization of cross-linked polymer coatings on the Cu stubs (e.g., replacing SU-8 with another type of polymer).

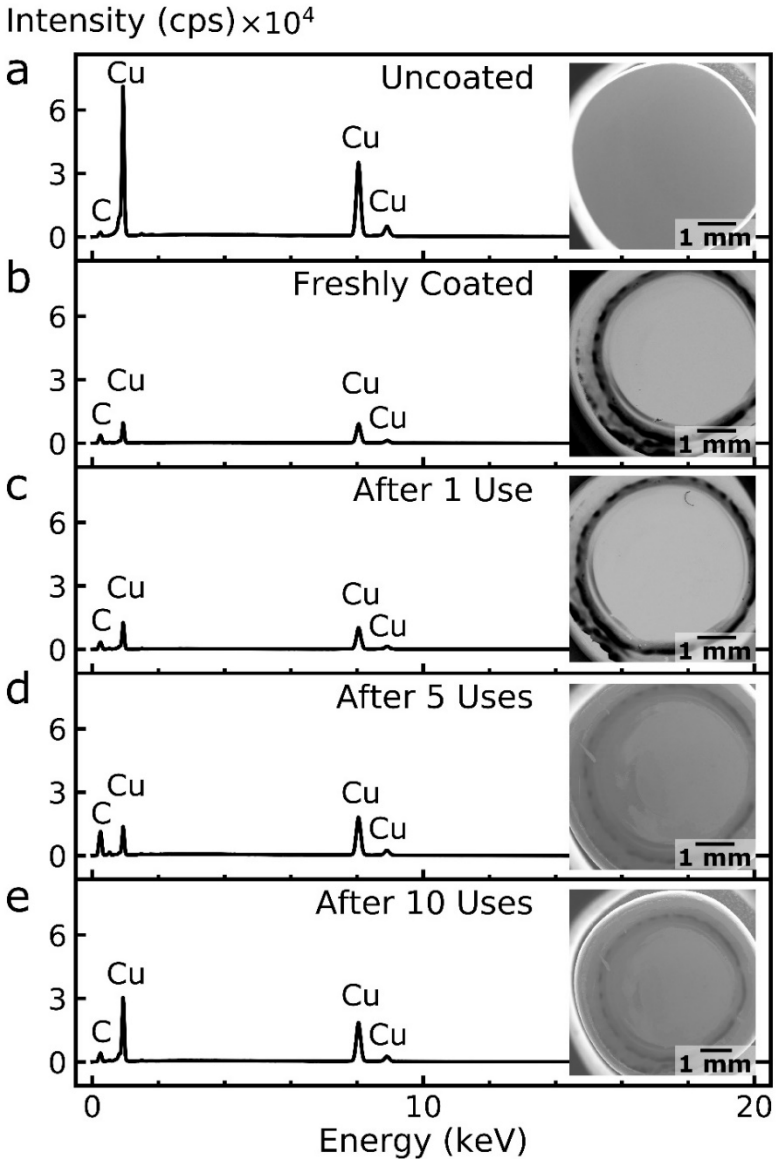

Figure 9. Representative plots of the EDS analyses of an SU-8 based polymer coated Cu stub used as a support for zeolite particles with corresponding SEM image inlays, depicting the polished Cu stub: (a) before it was coated with an SU-8 based polymer; (b) after it was coated with a cross-linked SU-8 film (i.e., "freshly coated"); and (c-e) after 1, 5, and 10 repetitions (i.e., uses) of a process of drop casting of ZSM-5 zeolite particles onto the stub and the subsequent removal of these particles (cleaning) by sonication, meant to demonstrate the reusability of these SU-8 based polymer coated Cu stubs.

Conclusions

It was demonstrated that a coating of cross-linked SU-8 on polished copper (Cu) stubs enabled the SEM and EDS analysis of ZSM-5 zeolite particles, specifically the Si and Al relative abundance in a particle. The process adopted to prepare the polymer coated stub enabled these analyses without interference from background Si or Al signals that are otherwise present in commonly used support materials during SEM sample preparation and analysis. The polymer coated Cu stubs were shown to be reusable for different samples up to nine times before the degradation of the polymer film was severe enough that complete removal of zeolite particles after characterization was not feasible. The degradation of the polymer film was attributed to the sonication step used to remove the previous sample material prior to re-using the polymer coated stub. The polymer coated Cu stub enabled an accurate determination of the shape, size, and Si:Al composition of the ZSM-5 zeolite particles and, therefore, no noticeable charging of the zeolite particles during electron beam characterization using SEM-based EDS analyses. These substrates could find applicability for the analysis of other Si and Al containing materials, as well as other types of non-conductive particles.

Competing Interests

The author(s) declare none.

Acknowledgements

This research was supported in part by the Natural Sciences and Engineering Research Council of Canada (NSERC; Grant No. RGPIN-2020-06522), an NSERC Canada graduate scholarship-doctoral (CGS-D) (A.M.K. Hadley), and CMC Microsystems (MNT Grant No. 10044). This work made use of the 4D LABS and the Center for Soft Materials shared facilities supported by the

Canada Foundation for Innovation (CFI), British Columbia Knowledge Development Fund (BCKDF), Western Economic Diversification Canada, and Simon Fraser University.

Data Availability

The Supplementary Materials are made available on-line.

References

1. Auerbach, S. M., Carrado, K. A., Dutta, P. K. (2005). *Part II: Synthesis and Structure in Handbook of Zeolite Science and Technology.* New York: Marcel Dekker, Inc, pp. 25-266.

2. Jamali, S. H., Vlugt, T. J. H., Lin, L-C. (2017). Atomistic Understanding of Zeolite Nanosheets for Water Desalination. *J. Phys. Chem. C.* **121***,* 11273−11280.

3. Ou, X., Xu, S., Warnett, J. M., Holmes, S. M., Zaheer, A., Garforth, A. A., Williams, M. A., Jiao, Y., Fan, X. (2017). Creating Hierarchies Promptly: Microwave-Accelerated Synthesis of ZSM-5 Zeolites on Macrocellular Silicon Carbide (SiC) Foams. *Chem. Eng. J.* **312***,* 1–9.

4. Cao, Z., Zeng, S., Xu, Z., Arvanitis, A., Yang, S., Gu, X., Dong, J. (2018). Ultrathin ZSM-5 Zeolite Nanosheet Laminated Membrane for High-Flux Desalination of Concentrated Brines. *Sci. Adv.* **4**: eaau8634.

5. Chao, P-Y., Hsu, C-H., Loganathan, A., Lin, H-P. (2018). One-Pot Synthesis of Sheet-Like MFI as High-Performance Catalyst for Toluene Disproportionation. *J. Am. Ceram. Soc.* **101**, 3719–3728.

6. Donato, L., Garofalo, A., Drioli, E., Alharbi, O., Aljlil, S. A., Criscuoli, A., Algieri, C. (2020). Improved Performance of Vacuum Membrane Distillation in Desalination with Zeolite Membranes. *Sep. Purif. Technol.* **237**, 116376.

7. Liu, Y., Qiang, W., Ji, T., Zhang, M., Li, M., Lu, J., Liu, Y. (2020). Uniform Hierarchical MFI Nanosheets Prepared via Anisotropic Etching for Solution-Based Sub–100-nm-Thick Oriented MFI Layer Fabrication. *Sci. Adv.* **6**: eaay5993.

8. Rehman, A. U., Arepalli, D., Alam, S. F., Kim, M-Z., Choi, J., Cho, C. H. (2021). Two-Dimensional MFI Zeolite Nanosheets Exfoliated by Surfactant Assisted Solution Process. *Nanomaterials.* **11***,* 2327.

9. Choi, M., Na, K., Kim, J., Sakamoto, Y., Terasaki, O., Ryoo, R. (2009). Stable Single-Unit-Cell Nanosheets of Zeolite MFI as Active and Long-Lived Catalysts. *Nature.* **461**, 246–249.

10. Varoon, K., Zhang, X., Elyassi, B., Brewer, D. D., Gettel, M., Kumar, S., Lee, J. A., Maheshwari, S., Mittal, A., Sung, C-Y., Cococcioni, M., Francis, L. F., McCormick, A. V., Mkhoyan, K. A., Tsapatsis, M. (2011). Dispersible Exfoliated Zeolite Nanosheets and Their Application as a Selective Membrane. *Science.* **334 (6052)**, 72-75.

11. Sabnis, S., Tanna, V. A., Li, C., Zhu, J., Vattipalli, V., Nonnenmann, S. S., Sheng, G., Lai, Z., Winter, H. H., Fan, W. (2017). Exfoliation of Two-Dimensional Zeolites in Liquid Polybutadienes. *Chem. Commun.* **53**, 7011.

12. Sari, Z. G. L. V., Younesi, H., Kazemian, H. (2015). Synthesis of Nanosized ZSM-5 Zeolite Using Extracted Silica from Rice Husk Without Adding Any Alumina Source. *Appl. Nanosci.* **5***,* 737-745.

13. Pérez-Page, M., Makel, J., Guan, K., Zhang, S., Tringe, J., Castro, R. H. R., Stroeve, P. (2016). Gas Adsorption Properties of ZSM-5 Zeolites Heated to Extreme Temperatures. *Ceram. Int.* **42***,* 15423-15431.

14. Medeiros-Costa, I. C., Laroche, C., Pérez-Pellitero, J., Coasne, B. (2019). Characterization of Hierarchical Zeolites: Combining Adsorption/Intrusion, Electron Microscopy, Diffraction and Spectroscopic Techniques. *Microporous Mesoporous Mater*. **287***,* 167-176.

15. Price, L. A., Ridley, C. J., Bull, C. L., Wells, S. A., Sartbaeva, A. (2021). Determining the Structure of Zeolite Frameworks at High Pressures. *Cryst. Eng. Comm.* **23***,* 5615.

16. Introduction to Energy Dispersive X-ray Spectrometry (EDS). https://cfamm.ucr.edu/media/126/download (accessed April 2022).

17. Silicon Wafers, Substrates and Specimen Supports. https://www.labtech-em.com/em/silicon-wafers-substrates-and-specimen-supports (accessed April 2022).

18. Janda, A., Bell, A. T. (2013). Effects of Si/Al Ratio on the Distribution of Framework Al and on the Rates of Alkane Monomolecular Cracking and Dehydrogenation in H-MFI. *J. Am. Chem. Soc.* **135 (51)**, 19193–19207.

19. Gao, Y., Zheng, B., Wu, G., Ma, F., Liu, C. (2016). Effect of the Si/Al Ratio on the Performance of Hierarchical ZSM-5 Zeolites for Methanol Aromatization. *RSC Adv.* **6**, 83581-83588.

20. Linder, V., Gates, B. D., Ryan, D., Parviz, B. A., Whitesides, G. M. (2005). Water-Soluble Sacrificial Layers for Surface Micromachining. *Small.* **1**, 730-736.

21. Wang, R., Cui, C., Zhang, C., Ren, C., Chen, G., Shao, T. (2018). Deposition of SiOx Film on Electrode Surface by DBD to Improve the Lift-Off Voltage of Metal Particles. *IEEE Trans. Dielectr. Electr. Insul.* **25(4)**, 1285-1292.

22. Berger, C., Phillips, R., Centeno, A., Zurutuza, A., Vijayaraghavan, A. (2017). Capacitive Pressure Sensing with Suspended Graphene–Polymer Heterostructure Membranes. *Nanoscale.* **9**, 17439-17449.

23. Bleiker, S. J., Dubois, V., Schröder, S., Stemme, G., Niklaus, F. (2017). Adhesive Wafer Bonding with Ultra-Thin Intermediate Polymer Layers. *Sens. and Actuators A Phys.* **260**, 16–23.

24. Barton, A. F. M. (1990). *Handbook of Polymer-Liquid Interaction Parameters and Solubility Parameters (1st ed.).* New York: Routledge.

25. Grande, C. D., Mangadlao, J., Fan, J., Leon, A. D., Delgado-Ospina, J., Rojas, J. G., Rodrigues, D. F., Advincula, R. (2017). Chitosan Cross-Linked Graphene Oxide Nanocomposite Films with Antimicrobial Activity for Application in Food Industry. *Macromol. Symp.* **374**, 1600114.

26. Kayaku Advanced Materials, "SU-8 2-25 Technical Data Sheet", September 2020, Ver. 1.

27. Bhushan, B. (2012). *Encyclopedia of Nanotechnology*. Dordrecht: Springer.

28. Carbon Tape (a). https://shilpent.com/other-products/48-carbon-tape.html (accessed January 2023).

29. Carbon Tape (b). https://www.techinstro.com/carbon-tape/ (accessed January 2023).

30. Hall, D. B., Underhill, P., Torkelson, J. M. (1998). Spin Coating of Thin and Ultrathin Polymer Films. *Polym. Eng. Sci.* **38(12)**, 2039-2045.

31. Gates, B. D., Xu, Q., Thalladi, V. R., Cao, T., Knickerbocker, T., Whitesides, G. M. (2004). Shear Patterning of Microdominos: a New Class of Procedures for Making Micro- and Nanostructures. *Angew. Chem. Int. Ed. Engl.* **43(21)**, 2780-2783.

32. Norrman, K., Ghanbari-Siahkali, A., Larsen, N. B. (2005). 6 Studies of Spin-Coated Polymer Films. *Annu. Rep. Prog. Chem., Sect. C: Phys. Chem.* **101**, 174-201.

33. Mouhamad, Y., Mokarian-Tabari, P., Clarke, N., Jones, R. A. L., Geoghegan, M. (2014). Dynamics of Polymer Film Formation During Spin Coating. *J. Appl. Phys.* **116**, 123513.

34. Lang, W. (1971). Nomarski Differential Interference-Contrast Microscopy. III. Comparison with Phase Contrast. *ZEISS Information*. **76**, 69-76.

35. Deegan, R. D., Bakajin, O., Dupont, T. F., Huber, G., Nagel, S. R., Witten, T. A. (1997). Capillary Flow as the Cause of Ring Stains from Dried Liquid Drops. *Nature.* **389***,* 827-829.

36. Mampallil, D., Eral, H. B. (2018). A Review on Suppression and Utilization of the Coffee-Ring Effect. *Adv. Colloid Interface Sci.* **252**, 38-54.

624 37. Zhang, Y., Chen, X., Liu, F., Li, L., Dai, J., Liu, T. (2018). Self-Assembled and Artificial
625 Surfaces/Interfaces: From Soft Matter to Metamaterials. *Adv. Condens. Matter Phys.*
626 **2018**, 9795654.
627
628 38. Yang, M., Chen, D., Hu, J., Zheng, X., Lin, Z-J., Zhu, H. (2022). The Application of
629 Coffee-Ring Effect in Analytical Chemistry. *TrAC, Trends Anal. Chem.* **157**, 116752.

630 39. Marica, I., Stefan, M., Boca, S., Falamaş, A., Farcău, C. (2023). A Simple Approach for
631 Coffee-Ring Suppression Yielding Homogeneous Drying Patterns of ZnO and TiO_2
632 Nanoparticles. *J. Colloid Interface Sci.* **635**, 117-127.

633 40. Widayat, W., Annisa, A. N. (2017). Synthesis and Characterization of ZSM-5 Catalyst at
634 Different Temperatures. *IOP Conf. Ser.: Mater. Sci. Eng.* **214**, 012032.

635 41. Li, T., Krumeich, F., Chen, M., Ma, Z., van Bokhoven, J. A. (2020). Defining
636 Aluminum-Zoning During Synthesis of ZSM-5 Zeolites. *Phys. Chem. Chem. Phys.* **22**,
637 734-739.

638 42. Yin, J-Y., Ma, L-Y., Siu, K-C., Wu, J-Y. (2019). Effects of Ultrasonication on the
639 Conformational, Microstructural, and Antioxidant Properties of Konjac Glucomannan.
640 *Appl. Sci.* **9(3)**, 461.